Journal of Molecular Catalysis A: Chemical 355 (2012) 180–185

Contents lists available at SciVerse ScienceDirect

Journal of Molecular Catalysis A: Chemical

journal homepage: www.elsevier.com/locate/molcata

A selective synthesis of 1-phenylethanol and γ-butyrolactone through coupling processes over Cu/MgO catalysts

Kannapu Hari Prasad Reddy, Narani Anand, Vakati Venkateswarlu, Kamaraju Seetha Rama Rao, David Raju Burri*

Catalysis Laboratory, I & PC Division, Indian Institute of Chemical Technology, Hyderabad 500 607, India

ARTICLE INFO

Article history:
Received 18 May 2011
Received in revised form
28 September 2011
Accepted 8 December 2011
Available online 17 December 2011

Keywords:
Hydrogen
Acetophenone
1-Phenylethanol
1,4-Butanediol
γ-Butyrolactone

ABSTRACT

A novel coupling route highlighting the combination of hydrogenation of acetophenone and dehydrogenation of 1,4-butanediol in vapor phase conditions over Cu–MgO catalyst is highly advantageous in terms of avoiding external pumping of H_2 and maintaining the formation of 1-phenylethanol and γ-butyrolactone, the desired products, respectively, in good amounts at atmospheric pressure. Three Cu/MgO catalysts with 5, 10, and 15 wt.% Cu loadings are prepared by impregnation method and characterized by BET surface area, temperature programmed reduction, XRD, N_2O pulse chemisorption, transmission electron microscopy (TEM) and X-ray photoelectron spectroscopy (XPS). Among the studied Cu/MgO catalysts, 10 wt.% Cu/MgO catalyst exhibited superior activity with nearly 100% selectivity of PhE and GBL. The higher yields of the products are observed on the 10 wt.% Cu/MgO in single and combined reactions compared to the other two catalysts, it may be due to the higher dispersion, smaller Cu particle size and more number of Cu^0/Cu^+ species at the surface.

1. Introduction

1-Phenylethanol (PhE) and γ-butyrolactone (GBL) are important chemicals and intermediates in fine chemicals industrial practices. PhE is mainly applied to produce perfumery products and pharmaceuticals [1]. GBL is mainly used for synthesis of N-vinylpyrrolidine, N-methylpyrrolidone, herbicides and rubber additives and a green solvent [2]. One of the important synthesis routes of PhE is the hydrogenation of acetophenone (ACP) and that of GBL is the dehydrogenation of 1,4-butanediol (BDO). Individual hydrogenation of ACP to produce PhE, ethylbenzene (EB), and 1-cyclohexylethanol (CHE) due to partially and fully reduction of carbonyl and phenyl groups of acetophenone. Several authors reported hydrogenation of ACP in liquid phase over supported metal catalysts [3–8], very few reports in vapor phase [9,10]. Selective production of PhE from ACP through catalytic transformation seems to be a challenging task. So far no vapor phase process is disclosed with 100% selectivity of PhE.

There are several reports for the production of GBL either from maleic anhydride hydrogenation or from BDO dehydrogenation using different heterogeneous catalysts, particularly copper based catalyst [11–15].

Apart from selective hydrogenation, in the coupled process, the hydrogen produced from the dehydrogenation reaction can be effectively utilized in the hydrogenation process with out purification. In spite of having the enormous importance of coupling processes, very few reports are available in the literature [2,16–22]. In addition the simplified coupling procedure due to a no-hydrogen-supply operation shows improved technology and environmentally benign process [17]. There is possibility of coupling of BDO and ACP. The dehydrogenation of BDO reaction has not been coupled with selective hydrogenation of ACP. Thus the detailed study of this coupling process shows great interest. A review article on catalytic transfer hydrogen highlight the application of various metal catalysts like Pd, Pt, Raney Ni, Ru, Ir, Rh for transfer hydrogenation olefins acetylenes, carbonyl compounds, nitriles, imines, azocompounds and nitro compounds, mostly in liquid phase [23]. The present study highlights the simultaneous synthesis of GBL and PhE by coupling BDO dehydrogenation and ACP hydrogenation over Cu/MgO catalysts in vapor phase.

2. Experimental

2.1. Catalyst preparation

MgO support is prepared by a precipitation method using Mg $(NO_3)_2{\cdot}6H_2O$ as a precursor and K_2CO_3 as a precipitating agent. 10 wt.% of aqueous Mg $(NO_3)_2{\cdot}6H_2O$ and K_2CO_3 solutions are prepared and mixed simultaneously at a constant pH of 9 until the precipitation completed. The precipitate is washed thoroughly with hot water until complete removal of K^+. The material dried and

* Corresponding author. Tel.: +91 40 27191712; fax: +91 40 27160921.
E-mail address: david@iict.res.in (D.R. Burri).

1381-1169/$ – see front matter © 2012 Elsevier B.V. All rights reserved.
doi:10.1016/j.molcata.2011.12.014

calcined at 723 K for 12 h. Three Cu/MgO catalysts with 5, 10, 15 wt.% Cu loadings are prepared by impregnation method using aqueous Cu $(NO_3)_2{\cdot}6H_2O$ solution. The catalysts are dried at 373 K for 12 h and calcined at 723 K for 12 h.

2.2. Catalyst characterization

BET surface areas are determined using a Smart Sorb 92/93(M/S.SMART Instrument, India). The detailed procedure reported elsewhere [2]. X-ray diffraction (XRD) measurements were made using a Rigaku Miniflex powder diffracts meter with Cu Kα radiation (40 kV, 30 mA). The copper surface area and the metal dispersion were estimated by nitrous oxide pulse chemisorption on pre-reduced catalysts under dynamic conditions [2]. Based on the stoichiometry, that one N_2O molecule requires two Cu atoms, the number of surface Cu species was estimated.

$$N_2O + 2Cu \rightarrow Cu_2O + N_2$$

The Cu dispersion (D_{Cu}) was measured as the percentage ratio of surface Cu atoms to the total number of Cu atoms present in the catalyst. Multiplying the number of surface Cu atoms with the cross sectional area of Cu ($6.803 \times 10^{-20}\ m^2$) gives the Cu-metal surface area per gram catalyst (S_{Cu}). The Cu particle size was estimated assuming a particle of cubic shape using the following equation:

$$Cu - particle\ \ size(P_{Cu})in\ \ nm = \frac{\%\ \ Cu\ \ loading \times 6 \times 10^3}{100 \times \rho \times S_{Cu}}$$

where ρ is the density of Cu metal ($8.92\ g\,cm^{-3}$).

Temperature programmed reduction (TPR) experiments were performed using a home made TPR system. The details are described elsewhere [2]. X-ray photoelectron spectroscopy (XPS) were recorded using a Kratos-Axis 165 instrument with Mg Kα radiation ($h\upsilon = 1253.6$ eV) at 75 W. Transmission electron micrographs (TEM) were recorded using a Phillips Tecnai G^2 FEI F12 electron microscope.

2.3. Catalytic activity tests

The catalytic experiments are carried out in a fixed bed reactor (10 mm i.d and 200 mm long) at atmospheric pressure. Around 0.5 g of catalyst is loaded and reduced in H_2 flow at 553 K for 3 h. Cu component in the catalyst is known to start sintering beyond 553 K. That is the reason why the reduction temperature is fixed at 553 K [2]. BDO and/or ACP are feed at a flow rate of 1 ml h^{-1} along with N_2 gas flow at a rate 18 ml min^{-1}. For independent ACP hydrogenation reaction H_2 is used a reducing gas. The feed composition of H_2:ACP is fixed at 1:1 with a space velocity ~100 m mol g^{-1}. In the combination reactions ACP to BDO ratio is maintained at 2:1 along with N_2 flow 18 ml min^{-1}. The product mixture is collected in an ice cold trap periodically for every 1 h and analyzed by GC (Shimadzu-17A) equipped with FID detector and ZB-wax capillary column (30 m $L \times 0.5$ mm I.D $\times$ 1 μm F.T). Prior to regular analysis, the products are identified by GC–MS (Shimadzu-QP 5050) equipped with DB-5 capillary column (30 m $L \times 0.32$ mm I.D $\times$ 1 μm F.T).

3. Results and discussion

The surface areas of the reduced catalysts are displayed in Table 1. There is a significant enhancement in the surface area of 10CMI catalyst compared to 5CMI catalyst. The enhancement in surface area with increase in Cu loading may be due to contribution of finely dispersed Cu species. The lowering in the surface area with increase in Cu loading from 10% to 15% may be due to agglomeration of some of the finely dispersed Cu species [2].

Table 1
BET surface area, dispersion, metal surface and particle size of reduced 5CMI, 10CMI, and 15CMI catalysts.

Catalyst	S_{BET} ($m^2\,g^{-1}$)	D_{Cu}[a] (%)	S_{Cu}[a] ($m^2\,g^{-1}$)	P_{Cu}[a] (nm)	P_{Cu}[b] (nm)
5CMI	13	5.5	4.2	32	16
10CMI	18	8.9	7.8	20	26
15CMI	11	3.8	2.9	46	35

S_{BET} is BET surface area, D_{Cu} is Cu-dispersion, S_{Cu} is Cu metal area and P_{Cu} is Cu particle size.
[a] Obtained from N_2O pulse chemisorption.
[b] Obtained from XRD.

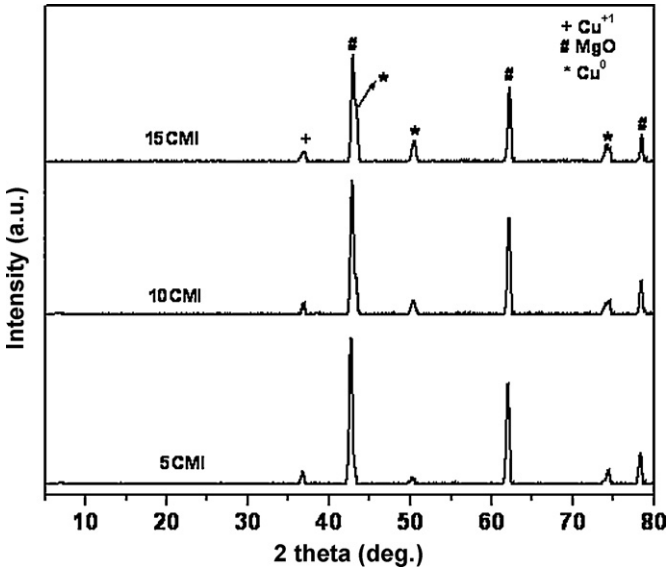

Fig. 1. XRD patterns of reduced 5CMI, 10CMI, and 15CMI catalysts.

N_2O pulse chemisorption is a valuable technique for the determination of (i) dispersion, (ii) metal surface area, and (iii) particle sizes of surface Cu species. The obtained N_2O pulse chemisorption data of all the Cu/MgO catalysts are shown in Table 1. Wherein, the dispersion of Cu metal and metal surface area is increased with increase in Cu loading from 5% to 10%, whereas, Cu particle size is decreased significantly. A reverse trend is observed in all the above stated parameters with the increase in Cu loading from 10% to 15%. Metal support interaction may be playing a crucial role in controlling the above parameters against Cu loading. The higher Cu dispersion in 10CMI catalyst is due to the Cu–MgO interaction. The presence of defect sites in MgO is the reason for the presence of such interacted species [24–26].

In Fig. 1, the X-ray powder diffraction patterns of reduced (553 K for 3 h) Cu/MgO catalysts are shown. The XRD reflections related to Cu^+ ($2\theta = 36.60^\circ$) and Cu^0 ($2\theta = 43.46^\circ$, 50.3° and 74.60°) along with MgO support (Mg^{2+}, $2\theta = 42.82$, 62.25, and 78.30°) are observed from the XRD patterns. No XRD reflections corresponding to Cu^{2+} are observed.

As shown in Table 1, the crystallite sizes of Cu from N_2O pulse chemisorption and from the XRD patterns of reduced catalysts are not matching. This is because of the fact that the reduced catalysts while recording for their XRD are exposed to air and therefore, there is a possibility that some part of Cu might have oxidized. The CuO thus formed due to areal oxidation may be in the amorphous form. On the other hand in situ reduction step is done prior to the N_2O pulse chemisorption and hence the crystallite sizes from these two techniques are not matching perfectly. Since our aim is to measure the Cu crystallite sizes, it is appropriate to use N_2O pulse chemisorption for the measurement of Cu crystallite sizes [2].

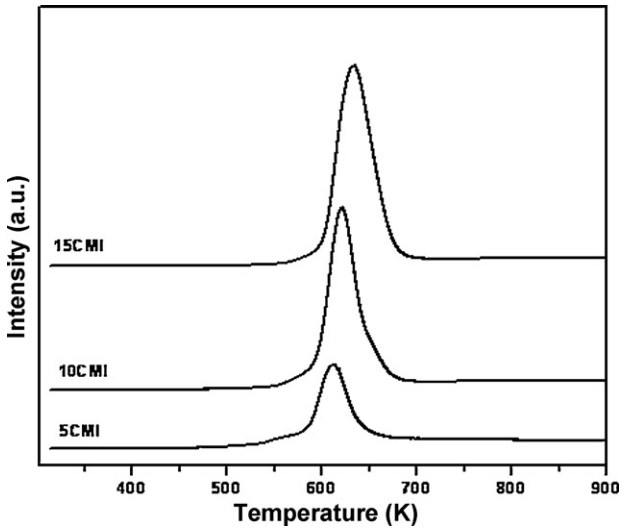

Fig. 2. TPR patterns of calcined 5CMI, 10CMI, and 15CMI catalysts.

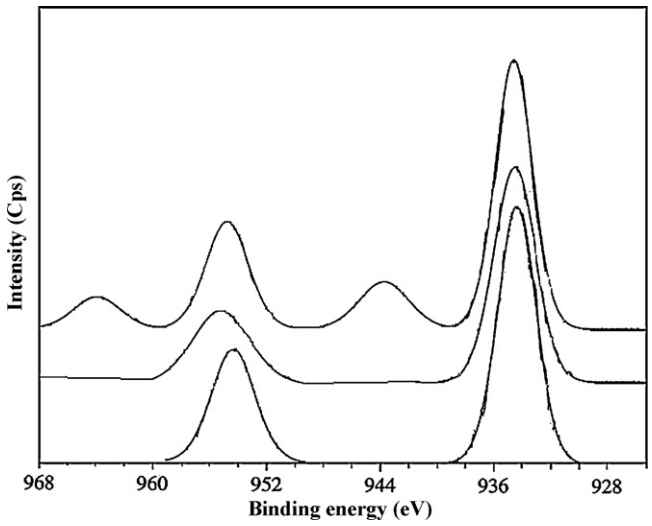

Fig. 4. XPS spectra of Cu 2p of 5CMI, 10CMI and 15CMI.

Fig. 2 implies the reducibility of Cu/MgO catalysts is determined by H_2-TPR. All the three Cu/MgO catalysts are shown a single reduction temperature maximum in the range of 610–640 K, which attribute to the reduction of CuO, similar to the reduction behavior of bulk CuO [27]. The reduction of CuO is started at around the reduction temperature of 500 K, which is extended up to 700 K with the increase in Cu loading from 5% to 15%, higher in reduction temperature maximum is observed (i.e. 5CMI → 610 K, 10CMI → 620 K, and 15CMI → 640 K). The lower reduction temperature attributed to the metal supported interaction and shifting of reduction temperature to higher indication of the attainment of CuO bulk nature. This result reveals that the copper dispersion is lower with higher copper loading, which is consistent with the results of N_2O pulse chemisorption, XRD, and the reported literature on supported copper catalysts CuO/Al_2O_3 [28].

TEM images and particle size distribution (bar diagram) of reduced catalysts are shown in Fig. 3. Cu particles are found to be well dispersed in 10 CMI (Fig. 3B) and the metal particles are found to be evenly distributed on the MgO support. However, in the case of 5CMI (Fig. 3A) catalyst the particle size of Cu metal is found to be large. The Cu metal particles are found to be agglomerated in 15 CMI (Fig. 3C). The average particle sizes of 5CMI, 10CMI and 15CMI are 32, 20 and 46 nm respectively.

The XPS patterns of reduced catalysts for Cu 2p are shown in Fig. 4. The corresponding characteristic of binding energy values of Cu 2p, Mg 2p, O 1s along with Cu_s/Cu_p (intensity ratio of the Cu 2p satellite peak to Cu 2p parent peak) and Cu/Mg atomic ratio are given in Table 2. The binding energy values of Cu $2p_{3/2}$ in 5CMI, 10CMI and 15CMI catalysts are found to be around 934.499 eV, 934.352 and 934.785 eV respectively; such values indicate the presence of copper in metallic form, as reported in the literature

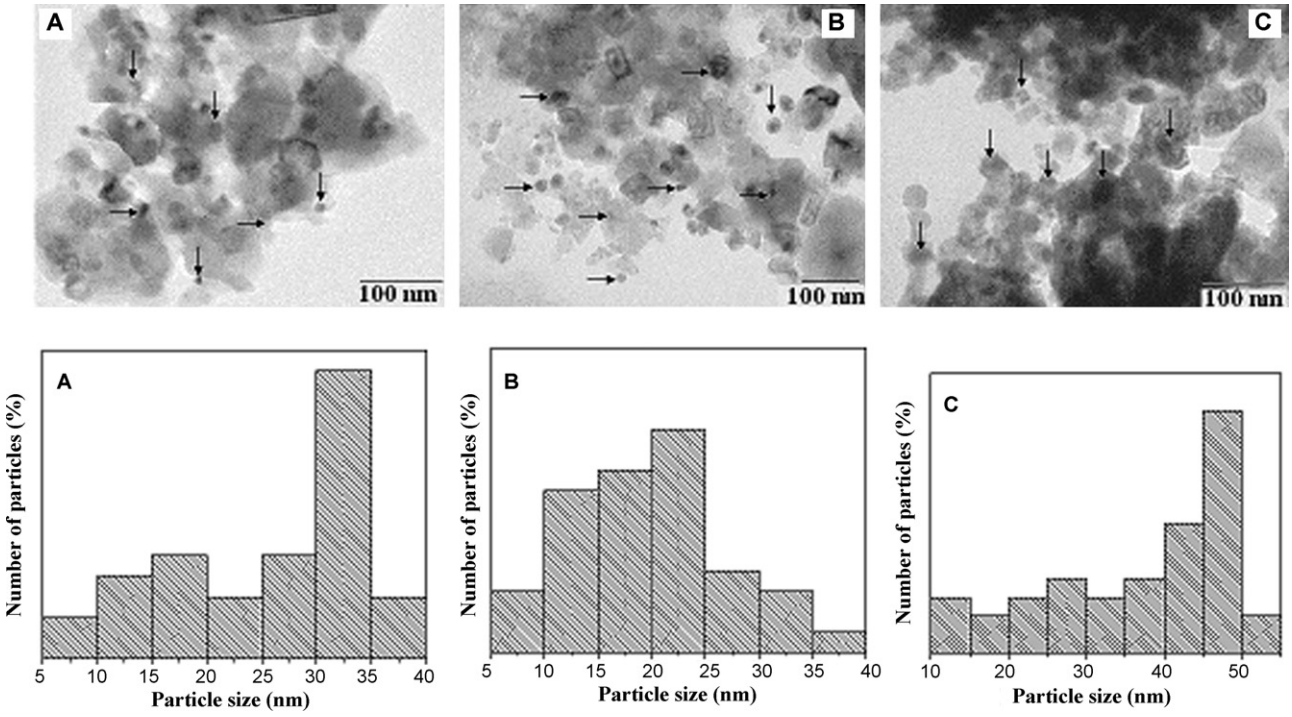

Fig. 3. TEM images of reduced catalysts (A) 5CMI, (B) 10CMI and (C) 15CMI.

Table 2
X-ray photoelectron spectroscopy of Cu–MgO catalysts.

Catalysts	Cu $2p_{3/2}$ parent (B.E.) eV	Cu $2p_{1/2}$ parent (B.E.) eV	Cu $2p_{3/2}$ satellite (B.E.) eV	Cu_s/Cu_p	Mg 2P (B.E.) eV	O 1S (B.E.) eV	Cu/Mg atomic ratio
5CMI	934.499	954.442	–	–	50.964	531.486	0.046
10CMI	934.352	954.324	–	–	50.337	531.385	0.110
15CMI	934.785	954.772	943.972	0.240	51.325	531.410	0.172

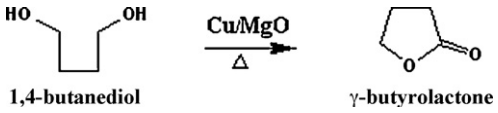

Scheme 1. Conventional dehydrogenation of BDO into GBL.

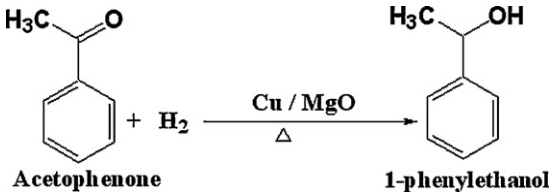

Scheme 2. Conventional hydrogenation of ACP to PhE.

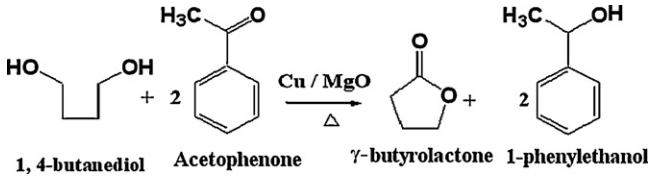

Scheme 3. Catalytic coupling of BDO dehydrogenation and acetophenone hydrogenation.

[22]. In the case of 5CMI, 10CMI catalysts no satellites are observed. It indicates copper species are presented in either in Cu^0/or Cu^+ state. But in the case of 15CMI catalyst satellite peak is observed at a binding energy of 943.97 eV. The satellite peaks shows in case of Cu^{+2} compounds are due to the shake up transitions by ligand to metal 3d charge transfer [29]. These satellite peaks are not seen in Cu^+ compounds or in metallic Cu because of completely filled 3d shells [30]. The surface composition of the Cu/MgO ratio (see in Table 2) is increasing with copper loadings, i.e. coverage of MgO support higher and surface area of the loaded catalysts decreasing with copper.

The O 1s and Mg 2p binding energy values (Table 2) are varied in all Cu/MgO catalysts. It indicates that metal supported interactions changed with copper loadings.

3.1. Catalytic activity

The advantage of catalytic coupling reactions is to avoid hydrogen pumping in the hydrogenation reaction. It was reported that cyclohexanol acts as a H_2 source (donor) for cholestanone hydrogenation to yield dihydrocholesterol over Raney nickel catalyst [23,31]. The selective vapor phase catalytic dehydrogenation of BDO to GBL can be expressed as follows (Scheme 1). In this reaction, 2 moles of hydrogen and 1 mol of GBL are produced. The selective hydrogenation of ACP to PhE can be expressed as in (Scheme 2). Wherein, 1 mol of hydrogen is required for the selective hydrogenation of ACP to PhE. The vapor phase catalytic hydrogenation–dehydrogenation coupling process is expressed as follows (Scheme 3). In this coupled process 1 mol of BDO and 2 mol of ACP convert into 1 mol of GBL and 2 mol of PhE. Interestingly, there are several reports for the selective production of GBL and hydrogen from BDO in the vapor phase [18,20]. However, selective production of PhE from ACP is a challenging task, because it involves a sequence of several competitive parallel and consecutive reactions [7]. It is reported that several Pt and Pd, and Ru based catalysts are selective, but operated at higher pressures and furthermore, the catalysts are highly expensive [9,10]. Of late, highly selective conversion of ACP to PhE is reported over Cu/SiO_2 catalysts [8], but high pressure operation and use of solvents are the disadvantages. Fortunately, in the present study, selective hydrogenation of ACP to PhE using in situ produced hydrogen has been achieved over Cu/MgO catalyst in the vapor phase and the details are in the proceeding sections.

3.1.1. Influence of Cu loading on MgO support on catalytic activity

The influence of Cu loading on MgO support in converting BDO and ACP into GBL and PhE respectively at a reaction temperature of 523 K can be seen from Table 3. There is a distinctive variation in the catalytic activity of three Cu/MgO catalysts. Among the three Cu/MgO catalysts 10CMI catalyst exhibited superior activity. Considerable hike in the conversion of BDO and ACP over 10CMI catalyst is observed. From Table 1 and Fig. 3, it is clear that the particle size of Cu in 10CMI is lower than those of 5CMI and 15CMI catalysts. More number of Cu sites and smaller particle size of Cu in 10CMI catalyst are collectively responsible for its higher activity both in BDO dehydrogenation to GBL and ACP hydrogenation to PhE.

3.1.2. Comparison of single and coupled process

BDO conversion and GBL selectivity in single and coupled processes are more or less similar, but there is a huge difference both in conversion of ACP and selectivity of PhE. The conversion of ACP is <6% over all the three catalysts in single reaction with external hydrogen source, when H_2:ACP =1:1 is maintained. In the coupled process, at same H_2 to ACP ratio, the conversion of ACP is about 8 times higher and also the selectivity of PhE is nearly 100%, which is a worth noting hydrogenation activity of Cu/MgO catalyst in the coupled process. Because, it is necessary to cease aromatic ring hydrogenation to avoid the formation of cyclohexyl related by-products and also impede further transformations of PhE [7]. The results (Table 3) reveal that the formation of 100% selectivity towards PhE is possible in the coupled process. To elucidate this significant result a mechanism is proposed (Scheme 4), wherein, BDO and ACP adsorb side by side on a single or adjacent two Cu sites as shown in step (A) and step (B) of Scheme 4. The proposed mechanism is partially related to both Rideal–Eley and Langmuir–Hinshelwood mechanisms. If BDO alone adsorbs on a single or neighboring dual Cu sites in single or coupled process, it behaves as a single reaction and yields GBL and H_2 (step C of Scheme 4). Similarly, if ACP alone adsorbs on a single or neighboring dual Cu sites in a single or coupled process, it is necessary to utilize hydrogen from the gaseous state to produce PhE, and proceeds as a single reaction. As shown in step (D) of Scheme 4, before desorbing PhE from Cu site, hydrogenolysis takes place to form ethyl benzene, and it depends on partial pressure of hydrogen [7]. In the independent ACP hydrogenation, the conversion of ACP is below 10% with ACP:H_2 mole ratio of 1:1. The selectivity of PhE is low in single reaction. Contrarily, in the coupled process due to competitive adsorption of BDO and ACP, the PhE depart from the catalyst surface as soon as it forms. In the coupled reaction, BDO:ACP mole ratio of 1:2 is maintained. With 0.64 fractional conversion of BDO,

Table 3
Catalytic activity of three Cu/MgO catalysts at 523 K.

Catalyst activity (%)	5CMI		10CMI		15CMI	
	Single	Coupled[a]	Single	Coupled[a]	Single	Coupled[a]
BDO conversion	40	35	70	64	32	26
GBL selectivity	98	100	99	100	99	100
ACP conversion[a]	3	30	6	44	1	23
PhE selectivity[a]	30	100	42	100	28	100

Catalyst = 0.5 g, feed mixture = 1 ml h^{-1}, N_2 = 18 ml min^{-1}.
[a] Stoichiometric quantity of BDO:ACP = 1:2, which is maintained in single reaction with H_2.

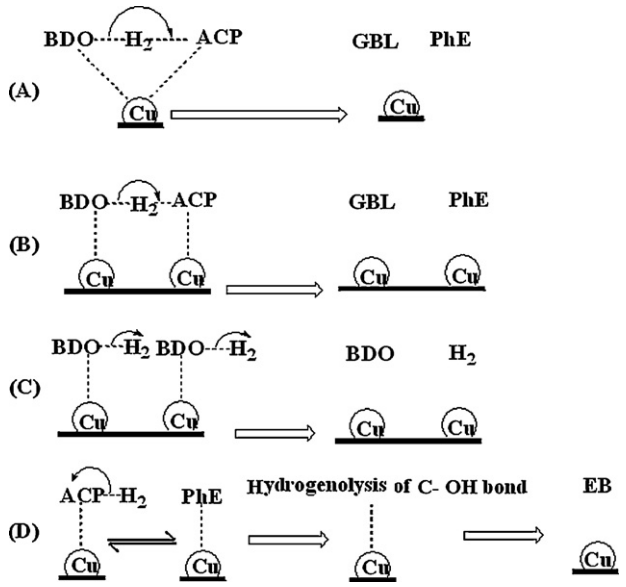

Scheme 4. Proposed reaction mechanism of BDO dehydrogenation and ACP hydrogenation coupling process.

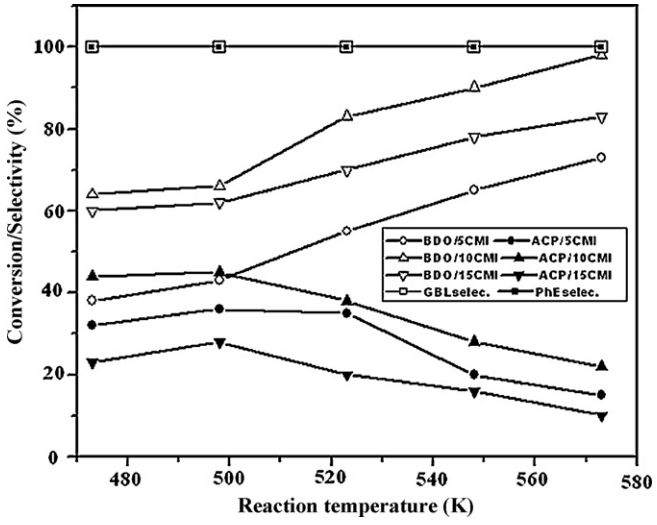

Fig. 5. Catalytic activity in the coupled process against reaction temperature over three Cu/MgO catalysts.

we can expect 1.28 moles of H_2 formation which is not sufficient to convert all the 2 moles of ACP. That is the reason why we got 0.44 mol of ACP conversion. However with this 0.44 mol of ACP conversion the H_2 required is 0.88 mol with left over 0.4 mol of H_2. The extra 0.4 mol of H_2 was observed at the outlet of the reactor in the gas phase. This H_2 is not taking part for further transformation.

3.1.3. Influence of reaction temperature in the coupled process

The activity of 5CMI, 10CMI, and 15CMI catalysts in the coupled BDO dehydrogenation and ACP hydrogenation at various reaction temperatures are conducted at atmospheric pressure in the vapor phase and the results are shown in Fig. 5. The enhancement in the BDO conversion and diminishing in the ACP conversion with increase in temperature appraises the endothermic and exothermic nature of BDO dehydrogenation and ACP hydrogenation. Formation of PhE from ACP is thermodynamically equilibrium controlled reaction, it leads to decrease the conversions at higher temperatures. However, the conversion of BDO, ACP over 10CMI catalyst is higher at all the reaction temperatures compared to 5CMI and 15CMI catalysts. In addition to its higher activity, 10CMI catalyst exhibited 100% selectivity towards GBL and PhE, which is a significant result in the selectivity point of view.

4. Conclusions

It can be concluded that the in situ production of hydrogen from 1,4-butanediol and its utilization for the selective production of 1-phenylethanol through catalytic coupling is achievable in the vapor phase over Cu/MgO catalysts. Higher Cu dispersion, and metal support interaction are responsible for higher activity of 10CMI catalyst. There is a lot of scope for the application of Cu catalysts for other coupling processes.

Acknowledgement

Hari Prasad Reddy, Anand and Venkateswarlu are thankful to Council of Scientific and Industrial Research (CSIR) New Delhi, for awarding research fellowships.

References

[1] Y. Kashiwagi, K. Uchiyama, F. Kurashima, C. Kikuchi, J. Anzai, Chem. Pharm. Bull. 47 (1999) 1051–1052.
[2] K. Hari Prasad Reddy, R. Rahul, S. Sree Vardhan Reddy, B. David Raju, K.S. Rama Rao, Catal. Commun. 10 (2009) 879–883.
[3] R.V. Malyala, C.V. Rode, M. Arai, S.G. Hegde, R.V. Chaudhari, Appl. Catal. A: Gen. 193 (2000) 71–86.
[4] M. Casagrande, L. Storaro, A. Talon, M. Lenarda, R. Frattini, E.R. Castellón, P.M. Torres, J. Mol. Catal. A: Chem. 188 (2002) 133–139.
[5] Y. Sun, Y. Guo, Q. Lu, X. Meng, W. Xiaohau, Y. Guo, Y. Wang, X. Liu, Z. Zhang, Catal. Lett. 100 (2005) 213–217.
[6] M. Lenarda, M. Casagrande, E. Moretti, L. Storaro, R. Frattini, S. Polizzib, Catal. Lett. 114 (2007) 79–84.
[7] J. Masson, P. Cividino, J. Court, Appl. Catal. A: Gen. 161 (1997) 191–197.
[8] N.M. Bertero, C.R. Apesteguıa, A.J. Marchi, Appl. Catal. A: Gen. 349 (2008) 100–109.
[9] C.-S. Chen, H.-W. Chen, Appl. Catal. A: Gen. 260 (2004) 207–213.
[10] C.-S. Chen, H.-W. Chen, W.-H. Cheng, Appl. Catal. A: Gen. 248 (2003) 117–218.
[11] Y.-L. Zu, J. Yang, G.-Q. Dong, H.-Y. Zheng, H.-H. Zhang, H.-W. Xiang, Y.-W. Li, Appl. Catal. B: Environ. 57 (2005) 183–190.
[12] K. Hari Prasad Reddy, N. Anand, P.S. Sai Prasad, K.S. Rama Rao, B. David Raju, Catal. Commun. 12 (2011) 866–869.
[13] H.E. Bellis, US Patent No. 5,110,954, 1992.
[14] R. Sigg, H. Regner, US Patent No. 5,426,195, 1995.
[15] H.J. Mercker, F.F. Pape, J. Simon, A. Henne, M. Hesse, U. Kohler, R. Dostalek, C. Freire, H. Krutz, US Patent No. 5,955,620, 1999.
[16] D. Zhang, H. Yin, R. Zhang, J. Xue, T. Jiang, Catal. Lett. 122 (2008) 176–182.

[17] H.Y. Zheng, Y.L. Zhu, Z.Q. Bai, L. Huang, H.W. Xiang, Y.W. Li, Green Chem. 8 (2006) 107–109.
[18] Y.L. Zhu, H.W. Xiang, Y.W. Li, H. Jiao, G.S. Wu, B. Zhong, G.Q. Guo, New J. Chem. 27 (2003) 208–210.
[19] A. Sun, Z. Qin, J. Wang, Catal. Lett. 79 (2002) 33–37.
[20] Y.L. Zhu, H.W. Xiang, G.S. Wu, L. Bai, Y.W. Li, Chem. Commun. 3 (2002) 254–255.
[21] K.S. Rama Rao, B. David Raju, S. Narayanan, B.M. Nagaraja, A.H. Padmasri, V. Siva Kumar, US patent No. 7015359B1, 2008.
[22] B.M. Nagaraja, A.H. Padmasri, P. Seetharamulu, K. Hari Prasad Reddy, B. David Raju, K.S. Rama Rao, J. Mol. Catal. A: Chem. 278 (2007) 29–37.
[23] G. Brieger, T.J. Nestrick, Chem. Rev. 74 (5) (1974) 567–580.
[24] C.T. Campbell, Surf. Sci. Rep. 27 (1997) 1–111.
[25] J.W. He, P.J. Moller, Surf. Sci. 180 (1987) 411–420.
[26] B.M. Nagaraja, V. Siva Kumar, V. Sashikala, A.H. Padmasri, B. Sreedhar, B. David Raju, K.S. Rama Rao, Catal. Commun. 4 (2003) 287–293.
[27] T. Nanba, S. Masukawa, J. Uchisawa, A. Obuchi, Catal. Lett. 93 (2004) 195–201.
[28] F.E. Lopez-Suarez, A. Bueno-Lopez, M.J. lllan-Gomez, Appl. Catal. B: Environ. 84 (2008) 651–658.
[29] K.S. Kim, J. Electron Spectrosc. Relat. Phenom. 3 (1974) 217–226.
[30] G. Avgouropoulos, T. Ioannides, Appl. Catal. A: Gen. 244 (2003) 155–167.
[31] E.C. Kleiderer, E.C. Kornfeld, J. Org. Chem. 13 (1948) 455–458.